SCIENCE CHINA
Chemistry

• ARTICLES •
• SPECIAL TOPIC • The Frontiers of Chemical Biology and Synthesis

January 2011 Vol.54 No.1: 31–42
doi: 10.1007/s11426-010-4176-8

Two remarkable epimerizations imperative for the success of an asymmetric total synthesis of (+)-aigialospirol

FIGUEROA Ruth[1], FELTENBERGER John B.[1], GUEVARRA Christle C.[1] & HSUNG Richard P.[1,2*]

[1]*Division of Pharmaceutical Sciences and Department of Chemistry, University of Wisconsin, Madison, WI 53705, USA*
[2]*School of Pharmaceutical Science and Technology, Tianjin University, Tianjin 300072, China*

Received July 29, 2010; accepted August 24, 2010

Two remarkable epimerization processes were uncovered during our pursuit of an enantioselective synthesis of (+)-aigialospirol featuring a cyclic acetal tethered ring-closing metathesis. Through modeling, we were able to turn these two unexpected epimerizations to our advantage via modeling to ensure a successful and concise total synthesis, thereby firmly establishing cyclic acetal tethered RCM as a powerful strategy in natural product synthesis. Most importantly, calculations allowed us to fully understand the nature and the mechanistic course of these two epimerizations that were imperative to the total synthesis efforts.

cyclic acetal, tethered RCM, (+)-aigialospirol, anomeric effect, and epimerization.

1 Introduction

In the last five years, we have been exploring chemistry of *cyclic acetals* [1, 2], which can serve either as an activator of 2π-components for cationic cycloadditions via vinyl oxocarbenium ions [3], or as a unique tether for intramolecular transformations that could lead to a useful strategy for constructing spiroketals (Figure 1) [4]. This program provided an invaluable opportunity for us to establish a fundamentally different, yet competitive, approach [5–7] compared to the classical spiroketal construction [4], while allowing us to explore the impact of the anomeric effect (~1.5 kcal/mol per anomeric effect) [8] on new reactivities [5, 9] and stereochemical issues [6, 9].

With exception of very few precedents [10–12], there have been no general studies on cyclic acetal tethered reactions to construct spiroketals. The lack of interest in using acetals as tethers could be due to their overwhelming reputation as protecting groups for carbonyls and alcohols and their perceived instability under hydrolytic conditions. However, we recognized that developing cyclic acetal tethered reactions would represent a fertile ground for discovering new synthetic strategies. Endeavors in pursuing strategies and approaches that are unconventional or even untapped have historically led to fertile grounds for uncov-

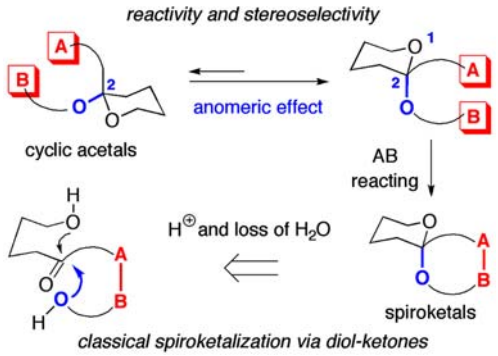

Figure 1 A cyclic acetal tethered strategy for spiroketal synthesis.

*Corresponding author (email: rphsung@pharmacy.wisc.edu)

ering new chemistry and for the advancement of synthesis.

Of all the methods that have been developed, cyclic acetal tethered RCM [13] appears to be the most powerful method (Scheme 1). Combining the prevalence of spiroketals in biologically active natural products [1, 2] and the power of RCM has rendered this a fundamentally different approach truly significant in natural product synthesis [7, 14]. More specifically, we became involved with the total synthesis of (+)-aigialospirol **4** [15] to demonstrate a point that the cyclic acetal tethered RCM strategy via **5** can lead to a competitive if not superior total synthesis than the classical spiroketal formation through diol-ketone **6**.

The isolation of (+)-aigialospirol **4** was reported by Isaka *et al*. [15]. It was obtained after an extended fermentation of the marine fungus *Aigialus parvus* BCC 5311 that was found in the mangrove Ascomycete. Although (+)-aigialospirol **4** has not been implicated with any biological activities [16], it is biosynthetically related to (+)-hypothemycin **7** [17–20], which was isolated from the same fungus source. (+)-Hypothemycin **7** is the well-known for its potent antimalarial [21] and anticancer [22] activities.

Specifically, **4** is postulated [15] to be derived from macro-lactone **8** via two steps, *trans*-lactonization and spiroketal formation. The macro-lactone **8** can be derived from a hydrative opening of the epoxide in **7** with inversion of

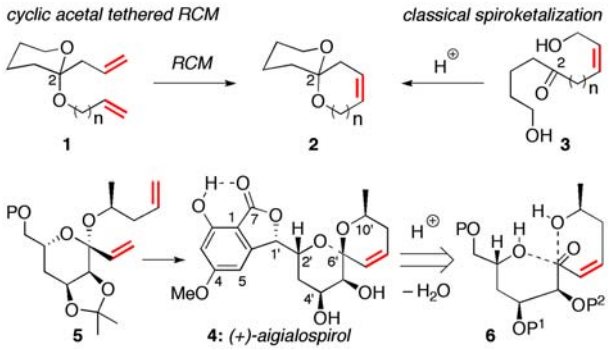

Scheme 1 A cyclic acetal tethered RCM.

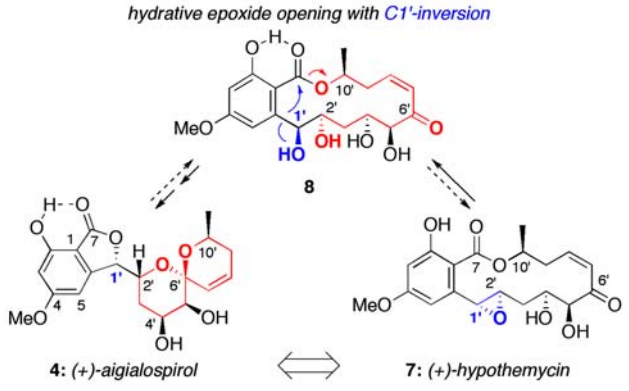

Scheme 2 Biosynthetic relation between (+)-aigialospirol and (+)-hypothemycin.

stereochemistry at C1′. Transformations in the reverse direction (**4** → **8** and **8** → **7**) are not known. We had recently completed the first total synthesis of (+)-aigialospirol **4** [23] featuring the cyclic acetal tethered RCM strategy. We wish to disclose here in this full paper two very interesting epimerizations that were key to the success of this total synthesis endeavor.

2 Experimental

2.1 General

All reactions were performed in flame-dried glassware under a nitrogen atmosphere. Solvents were distilled prior to use. Reagents were used as purchased (Aldrich, Acros), except where noted. Chromatographic separations were performed using Bodman 60 Å SiO_2. ^1H and ^{13}C NMR spectra were obtained on Varian VI-300, VI-400, and VI-500 spectrometers using $CDCl_3$ (except where noted) with TMS or residual $CHCl_3$ in the solvent as standard. Melting points were determined using a Laboratory Devices MEL-TEMP and are uncorrected/calibrated. Infrared spectra were obtained using NaCl plates on a Bruker Equinox 55/S FT-IR Spectrophotometer, and relative intensities are expressed qualitatively as s (strong), m (medium), and w (weak). TLC analysis was performed using Aldrich 254 nm polyester-backed plates (60 Å, 250 μm) and visualized using UV and a suitable chemical stain. Low-resolution mass spectra were obtained using an Agilent-1100-HPLC/MSD and can be either APCI or ESI, or an IonSpec HiRes-MALDI FT-Mass Spectrometer. High-resolution mass spectral analyses were performed at University of Wisconsin Mass Spectrometry Laboratories. All spectral data obtained for new compounds are reported. X-ray analyses were performed at the X-ray facility at University of Minnesota.

2.2 Experimental procedures and characterizations

*Synthesis of δ-lactone **9***

δ-Lactone **9** was prepared from *(S)*-glycidol in 6 steps with an overall yield of 42% yield (1.28 g) [23].

R_f = 0.11 (10% EtOAc in hexanes); On occasions, δ-lactone **9** solidifies into a white solid upon standing: mp 71–72 °C; $[\alpha]_D^{20} = -27.6$ (*c* 0.71, $CHCl_3$); ^1H NMR (400 MHz, $CDCl_3$) δ 1.06 (s, 9H), 1.38 (s, 3H), 1.49 (s, 3H), 2.03 (ddd, *J* = 15.0, 10.5, 3.5 Hz, 1H), 2.11 (dt, *J* = 15.0, 2.5 Hz, 1H), 3.77 (dd, *J* = 11.1, 3.9 Hz, 1H), 3.86 (dd, *J* = 11.3, 4.5 Hz, 1H), 4.59 (d, *J* = 6.8 Hz, 1H), 4.63–4.71 (m, 2H), 7.37–7.46 (m, 6H), 7.64–7.68 (m, 4H); ^{13}C NMR (125 MHz, $CDCl_3$) δ 19.5, 24.3, 26.3, 27.0, 30.6, 65.2, 71.9, 73.1, 75.4, 110.9, 128.0, 130.1, 132.9, 133.2, 135.7, 135.8, 168.3; IR (neat) cm^{-1} 2932w, 2857w, 1749m, 1472w, 1427m, 1376m, 1260m, 1209m, 1139m, 1110m, 1068m, 1041m, 1005m, 945m, 871w, 822m, 802m, 737m, 701s; HRMS (MALDI) calcd

for $C_{25}H_{32}O_5NaSi$ 463.1911, found 463.1906.

*Synthesis of lactol **10***

To a solution of δ-lactone **9** (534.0 mg, 1.21 mmol) in Et_2O (9 mL) was added vinyl magnesium bromide (1.0 M in THF: 1.30 mL, 1.30 mmol, 1.07 equiv) carefully dropwise at −78 °C. The pale yellow solution was stirred at −78 °C for 1 h before it was quenched with sat aq NH_4Cl at that temperature. H_2O was then added until all precipitate was dissolved. The resulting mixture was allowed to reach rt and was diluted with Et_2O. The aqueous phase was separated and extracted with two portions of Et_2O. The combined organic extracts were dried ($MgSO_4$) and concentrated *in vacuo* to give a cloudy crude oil that was purified via silica gel flash column chromatography (eluted with 10% EtOAc/90% hexane) to afford a mixture of lactol **10** and vinyl ketone **11** in 88% combined yield (500.0 mg) as a colorless oil.

R_f = 0.20 [10% EtOAc in hexanes]; $[\alpha]_D^{20}$ = −9.82 (*c* 2.50, $CHCl_3$); ^{1}H NMR (400 MHz, C_6D_6) δ 1.07 (s, 3H), 1.14 (s, 9H), 1.16 (s, 12H), 1.169 (s, 9H), 1.171 (s, 3H), 1.41 (s, 3H), 1.45 (s, 3H), 1.49 (s, 3H), 1.65–1.78 (m, 3H), 1.87 (dt, *J* = 14.2, 3.9 Hz, 1H), 2.07 (dt, *J* = 14.6, 2.7, Hz, 1H), 2.54 (dt, *J* = 14.5, 11.9, 3.0 Hz, 1H), 2.77–2.78 (m, 1H), 2.91–2.92 (m, 1H), 3.28–3.29 (m, 1H), 3.41 (dd, *J* = 10.6, 0.9 Hz, 1H), 3.59–3.78 (m, 5H), 3.93–4.00 (m, 1H), 4.11 (d, *J* = 8.0 Hz, 2H), 4.26–4.35 (m, 4H), 4.39 (d, *J* = 7.6 Hz, 1H), 4.42 (dt, *J* = 7.8, 2.7 Hz, 1H), 5.09 (dd, *J* = 10.5, 1.7 Hz, 1H), 5.17 (dd, *J* = 10.7, 1.8 Hz, 1H), 5.19 (dd, *J* = 10.3, 1.9 Hz, 1H), 5.64 (dd, *J* = 17.3, 1.7 Hz, 1H), 5.66 (dd, *J* = 17.2, 1.8 Hz, 1H), 6.00 (dd, *J* = 17.2, 10.5 Hz, 1H), 6.24 (dd, *J* = 17.3, 1.9 Hz, 1H), 6.40 (dd, *J* = 17.3, 10.6 Hz, 1H), 6.73 (dd, *J* = 17.3, 10.5 Hz, 1H), 7.27–7.18 (m, 18H), 7.74–7.83 (m, 12H); IR (neat) cm^{-1} 3441w, 2931w, 2857w, 1753w, 1697w, 1472w, 1427w, 1373w, 1262m, 1210m, 1110s, 1065m, 1041m, 701s; HRMS (MALDI) calcd for $C_{27}H_{36}O_5NaSi$ 491.2224, found 491.2229.

Preparations of cyclic acetals

Note: Two batches of (each batch 573.6 mg of the mixture **10** and **11**) the same amount was done and combined during the purification process. A round-bottomed flask was charged with the mixture of **10** and **11** (573.6 mg, 1.22 mmol), CH_2Cl_2 (13 mL), activated pulverized 4 Å molecular sieves (1.10 g) and chiral homo-allylic alcohol **12** [24, 25] (1.05 g, 12.24 mmol). The mixture was cooled to −78 °C and a solution of Tf_2NH (344.1 mg, 1.22 mmol) in CH_2Cl_2 (13 mL) was added via syringe (Note: This solution was freshly made prior to be used). The reaction mixture was stirred for 1 h before it was quenched with Et_3N (10 mL). The cooling bath was removed and the mixture was allowed to reach rt. After filtration through a pad of Celite^{TM}, the filtrate was concentrated *in vacuo* to give a crude yellow oil. At this point, the two identical batches were combined and purified via silica gel flash column chromatography (eluted with 5% EtOAc in hexanes) to afford cyclic acetal **14** in 76% yield (1.01 g) as a colorless oil.

R_f = 0.23 (5% EtOAc in hexanes); $[\alpha]_D^{20}$ = +3.85 (*c* 1.82, CH_2Cl_2); ^{1}H NMR (500 MHz, C_6D_6) δ 1.08 (d, *J* = 6.3 Hz, 3H), 1.16 (s, 3H), 1.18 (s, 9H), 1.43 (s, 3H), 1.87 (dt, *J* = 12.4, 1.5 Hz, 1H), 2.13–2.24 (m, 3H), 3.74 (dd, *J* = 10.5, 5.6 Hz, 1H), 3.94 (dd, *J* = 10.4, 5.6 Hz, 1H), 4.06–4.12 (m, 1H), 4.24 (d, *J* = 7.6 Hz, 1H), 4.49 (dd, *J* = 7.4, 2.6 Hz, 1H), 4.56 (dtd, *J* = 10.7, 5.6, 2.0 Hz, 1H), 4.91–4.99 (m, 2H), 5.28 (dd, *J* = 8.8, 3.9 Hz, 1H), 5.68 (ddt, *J* = 17.2, 10.1, 7.1 Hz, 1H), 5.77–5.86 (m, 2H), 7.22–7.24 (m, 6H), 7.80–7.85 (m, 4H); ^{13}C NMR (125 MHz) δ In C_6D_6: 19.5, 21.5, 24.0, 26.6, 27.1, 31.0, 43.0, 66.9, 68.1, 69.6, 70.9, 76.6, 98.5, 108.3, 117.1, 118.1, 128.1, 130.0, 133.9, 134.1, 135.3, 136.07, 136.15, 138.3 (missing two aryl carbons due to overlap); in $CDCl_3$: 19.6, 21.5, 24.2, 26.5, 27.1, 30.8, 42.7, 66.9, 67.7, 69.3, 70.8, 76.3, 98.0, 108.5, 117.3, 118.5, 127.9, 128.0, 129.9, 133.8, 133.9, 135.0, 135.9, 136.0, 137.7 (missing one aryl carbon due to overlapping *para*-carbons of the TBDPS group at 129.9 ppm); IR (neat) cm^{-1} 3073w, 2930m, 2859w, 1375w, 1263w, 1212m, 1107s, 1053s, 998s, 824m, 703s; HRMS (MALDI) calcd for $C_{32}H_{44}O_5NaSi$ 559.2850, found 559.2821.

Cyclic acetal **13:** R_f = 0.52 (20% EtOAc in hexanes); $[\alpha]_D^{20}$ = +10.52 (*c* 1.1, $CHCl_3$); ^{1}H NMR (400 MHz, C_6D_6) δ 7.78–7.85 (m, 4H), 7.20–7.25 (m, 6H), 5.84 (dd, 1H, *J* = 17.2, 10.4 Hz), 5.75 (dd, 1H, *J* = 7.2, 5.2 Hz), 5.70 (dd, 1H, *J* = 7.2, 5.2 Hz), 5.29 (dd, 1H, *J* = 10.4, 2.4 Hz), 5.03 (dt, 1H, *J* = 2.0, 1.2 Hz), 4.95 (ddt, 1H, *J* = 9.2, 1.2, 0.8 Hz), 4.49 (m, 2H), 4.23 (d, 1H, *J* = 7.6 Hz), 3.78 (m, 2H), 3.62 (dt, 1H, *J* = 9.6, 6.8 Hz), 3.46 (dt, 1H, *J* = 9.6, 6.8 Hz), 2.23 (ddd, 1H, *J* = 14.0, 12.4, 3.6 Hz), 2.17 (q, 2H, *J* = 6.8 Hz), 1.84 (dt, 1H, *J* = 14.0, 2.0 Hz), 1.44 (s, 3H), 1.17 (s, 9H), 1.15 (s, 3H); ^{13}C NMR (100 MHz, C_6D_6) δ 137.8, 136.2, 136.2, 136.1, 134.2, 134.0, 130.0, 130.0, 118.3, 116.3, 108.5, 98.6, 76.8, 71.0, 69.5, 68.1, 60.6, 34.9, 30.3, 27.2, 26.5, 23.9, 19.6; IR (neat) cm^{-1} 3072w, 2931m, 2858m, 2360w, 1782m, 1685w, 1428m, 1262m, 1210m, 1111s, 1061s, 997s; HRMS (ESI) calcd for $C_{31}H_{42}O_5Si$ 545.2699, found 545.2711.

Cyclic acetal tethered RCM

To a purple solution of the Grubbs' first generation catalyst (129.0 mg, 0.157 mmol) in toluene (270 mL) was added a solution of cyclic acetal **14** (676.0 mg, 1.26 mmol) in toluene (60 mL). The mixture was stirred at rt for 3 h. Subsequently, it was concentrated *in vacuo* to give a crude brown oil that was purified via silica gel flash column chromatography (eluted with 5% EtOAc in hexanes) to yield the pure spiroketal **16** in 86% yield (554.0 mg) as a colorless oil.

R_f = 0.20 (5% EtOAc in hexanes); $[\alpha]_D^{20}$ = +20.9 (*c* 0.77, $CHCl_3$); ^{1}H NMR (500 MHz, C_6D_6) δ 1.03 (d, *J* = 6.3 Hz, 3H), 1.17 (s, 9H), 1.23 (s, 3H), 1.52 (s, 3H), 1.58–1.68 (m, 3H), 2.06 (ddd, *J* = 14.1, 3.4, 2.2 Hz, 1H), 2.32 (ddd, *J* = 14.4, 11.7, 3.2 Hz, 1H), 3.64–3.70 (m, 1H), 3.83 (dd, *J* = 10.1, 6.2 Hz, 1H), 3.92 (dd, *J* = 10.0, 4.9 Hz, 1H), 4.42 (dt,

J = 7.6, 2.7 Hz, 1H), 4.48–4.53 (m, 1H), 5.68 (ddd, J = 10.3, 4.6, 3.7 Hz, 1H), 6.18 (dt, J = 10.3, 2.0 Hz, 1H), 7.15–7.21 (m, 6H), 7.79–7.83 (m, 4H); ^{13}C NMR (125 MHz) δ In C_6D_6: 19.6, 21.9, 24.3, 26.6, 27.2, 28.8, 31.1, 68.0, 68.6, 69.5, 71.1, 75.3, 95.3, 108.9, 126.3, 129.2, 129.82, 129.84, 134.3, 134.4, 136.1, 136.2 (missing two aryl carbons due to overlap); in $CDCl_3$: 19.6, 22.0, 24.5, 26.5, 27.2, 28.6, 31.2, 68.0, 68.2, 69.2, 70.9, 75.1, 95.1, 109.1, 127.7, 127.8, 127.9, 128.0, 129.7, 129.8, 134.1, 135.9, 136.0 (missing one aryl carbon due to overlapping Si-substituted *ipso*-carbons of the TBDPS group at 129.9 ppm); IR (neat) cm^{-1} 3071w, 3050w, 2931m, 1428w, 1371m, 1262w, 1210m, 1166m, 1139m, 1111s, 1032s, 823m, 700s; HRMS (MALDI) calcd for $C_{30}H_{40}O_5NaSi$ 531.2537, found 531.2550.

Spiroketal **15:** R_f = 0.53 (20% EtOAc in hexanes); $[\alpha]_D^{20}$ = −17.69 (*c* 0.9, $CHCl_3$); ^{1}H NMR (400 MHz, C_6D_6) δ 7.83 (m, 4H), 7.22 (m, 6H), 6.28 (ddd, 1H, J = 10.4, 2.8, 1.6 Hz), 5.71 (ddd, 1H, J = 10.4, 5.6, 1.6 Hz), 4.50 (ddd, 1H, J = 7.6, 2.8, 2.0 Hz), 4.45 (ddd, 1H, J = 10.8, 3.2, 1.6 Hz), 4.13 (d, 1H, J = 7.6 Hz), 3.95 (ddd, 1H, J = 12.0, 11.6, 3.6 Hz), 3.79 (ddd, 2H, J = 19.2, 10.4, 5.2 Hz), 3.44 (dd, 1H, J = 10.8, 6.4 Hz), 2.44 (ddd, 1H, J = 14.4, 8.8, 2.8 Hz), 1.98 (m, 1H), 1.91 (ddd, 1H, J = 14.0, 2.8, 2.0 Hz), 1.51 (s, 3H), 1.18 (s, 12H); ^{13}C NMR (100 MHz, C_6D_6) δ 136.2, 136.1, 134.3, 134.1, 130.0, 129.9, 128.9, 128.3, 128.1, 128.0, 127.8, 127.5, 108.8, 93.9, 76.7, 71.1, 69.4, 68.5, 57.7, 29.1, 27.2, 26.5, 24.9, 24.1, 19.6; IR (neat) cm^{-1} 3071w, 2932m, 2859w, 1473m, 1381m, 1371m, 1266m, 1138s, 1028s; HRMS (ESI) calcd for $C_{29}H_{38}O_5Si$ 494.6950, found 494.6950.

*Hydrolytic epimerization of spiroketal **16***

To a solution of spiroketal **16** (9.00 mg, 0.018 mmol) in MeOH (1 mL) was added *p*-TsOH (0.50 mg, 0.0027 mmol, practical grade). The mixture was stirred at rt for 1 h until TLC showed completion consumption of **16**. (Note: The reaction time varied, and thus, it should be carefully monitored via TLC analysis.) The reaction mixture was concentrated *in vacuo* and diluted with CH_2Cl_2 (10 mL). The resulting solution was washed with sat aq $NaHCO_3$ (1 mL). The aqueous layer was extracted with CH_2Cl_2 (3 × 5 mL). The combined organic layers were dried ($MgSO_4$) and concentrated *in vacuo* to afford a crude residue that was purified via silica gel flash column chromatography (eluted with 2% MeOH in CH_2Cl_2) to afford diol **17** in 81% yield (6.70 mg) as a white solid.

R_f = 0.16 (2% MeOH in CH_2Cl_2); mp 43–45 °C; $[\alpha]_D^{20}$ = +51.8 (*c* 0.62, CH_2Cl_2); ^{1}H NMR (500 MHz, C_6D_6) δ 0.90 (d, J = 6.3 Hz, 3H), 1.17 (s, 9H), 1.39–1.48 (m, 2H), 1.62 (ddt, J = 17.6, 11.0, 2.4 Hz, 1H), 1.91 (ddd, J = 13.9, 3.4, 2.4 Hz, 1H), 2.61 (d, J = 10.9 Hz, 1H), 3.30 (dd, J = 10.4, 3.4 Hz, 1H), 3.49 (d, J = 10.6 Hz, 1H), 3.65 (dd, J = 10.6, 4.3 Hz, 1H), 3.74 (dd, J = 10.6, 5.7 Hz, 1H), 3.98 (dqd, J = 10.9, 6.3, 3.3 Hz, 1H), 4.05–4.09 (m, 1H), 4.14–4.19 (m, 1H), 5.56 (ddd, J = 10.0, 2.7, 1.3 Hz, 1H), 5.72 (ddd, J = 10.0, 5.9, 1.9 Hz, 1H), 7.22–7.24 (m, 6H), 7.80–7.84 (m, 4H); ^{13}C NMR (125 MHz) δ In C_6D_6: 19.6, 20.8, 27.1, 31.7, 35.2, 64.5, 65.5, 67.2, 69.3, 71.4, 99.3, 128.4, 129.1, 129.99, 130.03, 134.10, 134.14, 136.16, 136.18; in $CDCl_3$: 19.6, 21.4, 27.1, 31.9, 35.3, 64.8, 65.3, 66.9, 71.3, 99.1, 127.5, 127.8, 127.9, 129.9, 130.0, 130.3, 133.8, 133.9, 135.9, 136.0; IR (CH_2Cl_2 film) cm^{-1} 3497br, 3047w, 2930m, 2857m, 1589w, 1427m, 1111s, 1066s, 1012s, 822m, 740m, 702s; HRMS (MALDI) calcd for $C_{27}H_{36}O_5NaSi$ 491.2224, found 491.2269.

*Synthesis of aldehyde **19***

To a solution of spiroketal **16** (138.5 mg, 0.27 mmol) in THF (10 mL) was added tetra-*n*-butylammonium fluoride (1.0 *M* in THF: 0.41 mL, 0.41 mmol). The resulting yellow solution was stirred at rt for 22 h. The mixture was concentrated *in vacuo* to give a crude residue that was purified via silica gel flash column chromatography (eluted with 35% EtOAc in hexanes) to afford the desired alcohol in 98% yield (72.3 mg) as a white solid.

R_f = 0.18 (35% EtOAc in hexanes); mp 131–134 °C; $[\alpha]_D^{20}$ = +108.9 (*c* 0.52, $CHCl_3$); ^{1}H NMR (400 MHz, C_6D_6) δ 0.97 (d, J = 6.1 Hz, 3H), 1.23 (d, J = 0.4 Hz, 3H), 1.44 (dddd, J = 17.1, 5.5, 3.8, 1.4 Hz, 1H), 1.52 (d, J = 0.4 Hz, 3H), 1.60 (ddt, J = 17.4, 9.1, 2.6 Hz, 1H), 1.64 (ddd, J = 14.4, 4.2, 2.6 Hz, 1H), 2.47 (ddd, J = 14.6, 12.0, 2.8 Hz, 1H), 2.83 (dd, J = 8.9, 2.6 Hz, 1H), 3.37 (ddd, J = 11.5, 8.8, 2.9 Hz, 1H), 3.55 (dqd, J = 9.3, 6.2, 3.6 Hz, 1H), 3.81 (dt, J = 11.4, 2.6 Hz, 1H), 3.97 (d, J = 7.7 Hz, 1H), 4.27–4.33 (m, 2H), 5.65 (ddd, J = 10.3, 5.7, 2.6 Hz, 1H), 6.13 (ddd, J = 10.3, 2.6, 1.4 Hz, 1H); ^{13}C NMR (125 MHz, C_6D_6) δ 21.5, 24.4, 25.4, 26.5, 31.1, 65.5, 68.4, 70.2, 70.8, 74.3, 95.5, 108.9, 126.8, 128.5; IR (neat) cm^{-1} 3447brw, 3050w, 2979w, 2921w, 1451w, 1431w, 1382m, 1370m, 1209m, 1168m, 1035s, 1016s; mass spectrum (APCI): *m*/*e* (% relative intensity) 271 (10) $(M + H)^+$, 253 (7) $([M+H]–H_2O)^+$, 227 (5), 213 (100), 195 (37), 167 (80); HRMS (ESI) calcd for $C_{14}H_{22}O_5NaSi$ 293.1365, found 293.1353.

To a solution of the above alcohol (117.1 mg, 0.43 mmol) in CH_2Cl_2 (4.6 mL) were added iodobenzene diacetate (153.5 mg, 0.48 mmol) and then 2,2,6,6-tetramethylpiperidine-1-oxyl (TEMPO) (8.50 mg, 0.054 mmol). The resulting orange solution was stirred at rt for 21 h before it was quenched with sat aq $Na_2S_2O_3$ (5.0 mL). The mixture was extracted with CH_2Cl_2 (3 × 10 mL), and the combined organic extracts were dried (Na_2SO_4) and concentrated *in vacuo* to give a yellow/orange oil that was purified via silica gel flash column chromatography (eluted with 15% EtOAc in hexanes to remove impurities and 30% EtOAc in hexanes) to afford aldehyde **19** in 78% yield (90.6 mg) as a white solid.

R_f = 0.66 (20% EtOAc in hexanes); mp 62–63 °C; $[\alpha]_D^{20}$ = +136.7 (*c* 0.73, $CHCl_3$); ^{1}H NMR (500 MHz, C_6D_6) δ 0.96 (d, J = 6.4 Hz, 3H), 1.18 (s, 3H), 1.46 (s, 3H), 1.56–1.59 (m, 2H), 2.04 (ddd, J = 14.4, 5.7, 2.8 Hz, 1H), 2.21 (ddd, J =

14.4, 11.1, 3.1 Hz, 1H), 3.52–3.58 (m, 1H), 3.84 (d, J = 7.4 Hz, 1H), 4.17 (dt, J = 7.6, 2.9 Hz, 1H), 4.34 (dd, J = 11.1, 5.7 Hz, 1H), 5.67 (ddd, J = 10.3, 4.7, 3.6 Hz, 1H), 6.14 (dt, J = 10.4, 2.0 Hz, 1H), 9.81 (s, 1H); ^{13}C NMR (125 MHz, C_6D_6) δ 21.5, 24.7, 25.3, 26.7, 30.9, 68.2, 70.3, 73.8, 75.1, 95.6, 109.3, 127.2, 127.8, 203.2; IR (neat) cm^{-1} 2984w, 2936w, 1735s, 1381s; mass spectrum (APCI): *m/e* (% relative intensity) 269 (15) $(M+H)^+$.

Preparation of amide ***20***

To a solution of 4-methoxysalicylic acid (2.52 g, 15.0 mmol) in DMF (12 mL) was added diisopropylethylamine (9.40 mL, 54.0 mmol) and *tert*-butyldimethylsilyl chloride (5.65 g, 37.5 mL). The mixture was vigorously stirred at rt for 3 h. The reaction mixture was poured over H_2O (30 mL) and extracted with Et_2O (4 × 50 mL). The combined organic extracts were washed with sat aq NaCl (2 × 25 mL), dried over $MgSO_4$, and concentrated *in vacuo* to yield a yellow oil that was purified via silica gel flash column chromatography (eluted with 2% EtOAc in hexanes) to afford the desired silyl ester in 74% yield (4.40 g) as a colorless oil.[26]

R_f = 0.21 (2% EtOAc in hexanes); ^{1}H NMR (400 MHz, $CDCl_3$) δ 0.19 (s, 6H), 0.32 (s, 6H), 0.97 (s, 9H), 0.99 (s, 9H), 3.78 (s, 3H), 6.37 (d, J = 2.5 Hz, 1H), 6.49 (dd, J = 8.8, 2.5 Hz, 1H), 7.75 (d, J = 8.8 Hz, 1H); ^{13}C NMR (100 MHz, $CDCl_3$) δ –4.4, –4.2, 18.0, 18.7, 26.0, 26.1, 55.5, 106.9, 107.5, 116.6, 133.7, 158.4, 163.7, 164.8; IR (neat) cm^{-1} 2954w, 2930w, 2858w, 1704m, 1606m, 1493w, 1463m, 1443m, 1337w, 1251s, 1169m, 1149m, 1134m, 1082s, 834s, 782s; HRMS (ESI) calcd for $C_{20}H_{37}O_4Si_2$ 397.2230, found 397.2221.

To a solution of the above silyl ester (250.0 mg, 0.630 mmol) in CH_2Cl_2 (0.6 mL) was added a drop of DMF. After cooling to 0 °C in an ice-water bath, oxalyl chloride (88.0 mg, 0.060 mL, 0.693 mmol) was added dropwise at a rate to maintain the control of the reaction. The resulting yellow solution was stirred 0 °C for 1.5 h before the ice bath was removed and the mixture was further stirred overnight. After which, the reaction mixture was concentrated *in vacuo*, re-diluted with fresh CH_2Cl_2, and re-concentrated *in vacuo* to afford the crude acyl chloride.

To a solution of the crude acyl chloride prepared above in CH_2Cl_2 (0.6 mL) was added diethylamine (93.0 mg, 0.13 mL, 1.26 mmol) at rt dropwise at a rate to maintain the control of the reaction. The resulting mixture was stirred for 1 h before being concentrated *in vacuo* to afford a crude residue that was purified via silica gel flash column chromatography (eluted with 20% EtOAc in hexanes) to yield the desired amide **20** in 56% yield (119.0 mg) as a colorless oil.

R_f = 0.41 (20% EtOAc in hexanes); ^{1}H NMR (400 MHz, $CDCl_3$) δ 0.22 (s, 6H), 0.96 (s, 9H), 1.01 (t, J = 7.1 Hz, 3H), 1.23 (t, J = 7.2 Hz, 3H), 3.10–3.34 (broad m, 2H), 3.34–3.70 (broad m, 2H), 3.78 (s, 3H), 6.36 (d, J = 2.3 Hz, 1H), 6.53 (dd, J = 8.5, 2.3 Hz, 1H), 7.12 (d, J = 8.4 Hz, 1H); ^{13}C NMR (100 MHz, $CDCl_3$) δ 13.5, 14.4, 18.3, 25.8, 39.5, 43.1, 55.5, 106.0, 106.5, 123.0, 128.8, 152.5, 160.9, 169.3 [missing two Me carbon resonances from the TBS group due to rotameric line broadening]; IR (neat) cm^{-1} 2933w, 2898w, 2860w, 1632brm, 1608brm, 1463brm, 1428br, 1288m, 1255m, 1166m, 839s, 783s; mass spectrum (APCI): *m/e* (% relative intensity) 338 (100) $(M+H)^+$; HRMS (MALDI) calcd for $C_{18}H_{32}O_3NSi$ 338.2146, found 338.2131.

Addition to aldehyde ***19***

To a round-bottomed flask charged with anhyd THF (1.2 mL) were added tetramethylethylenediamine (19.8 mg, ~0.030 mL, 0.17 mmol) and *s*-BuLi (1.4 M in cyclohexane: 0.12 mL, 0.17 mmol) at –78 °C via syringe. The deep yellow solution was stirred for 2 min before a solution of amide **20** (57.6 mg, 0.17 mmol) in THF (0.3 mL) was added dropwise also via syringe. The pale yellow solution was stirred for 45 min at –78 °C before a solution of aldehyde **19** (41.6 mg, 0.155 mmol) in THF (0.3 mL) was added. Additional THF (0.2 mL) was used to ensure complete transferred of the aldehyde. The mixture was stirred for 1 h at –78 °C and 2.5 h at rt, and it was quenched with H_2O (3 mL) and extracted with Et_2O (3 × 5 mL). The combined organic layers were dried (Na_2SO_4) and concentrated *in vacuo* to give a crude mixture that was purified via silica gel flash column chromatography (eluted with 10%–60% EtOAc in hexanes) to afford secondary alcohols **21**-*syn* (18.5 mg) and **21**-*anti* (28.8 mg) in a combined 50% yield.

21-*syn*: colorless thick oil; R_f = 0.34 (35% EtOAc in hexanes); ^{1}H NMR (400 MHz, C_6D_6) δ 0.15 (s, 3H), 0.21 (s, 3H), 0.79 (t, J = 7.1 Hz, 3H), 0.98 (s, 9H), 0.99 (d, J = 6.2 Hz, 3H), 1.09 (t, J = 7.1 Hz, 3H), 1.19 (s, 3H), 1.34–1.40 (m, 1H), 1.55 (s, 3H), 1.62 (ddt, J = 13.6, 9.8, 2.3 Hz, 1H), 1.86–1.90 (m, 1H), 2.52–2.58 (m, 1H), 2.94 (q, J = 7.1 Hz, 2H), 3.10 (sextet, J = 7.2 Hz, 1H), 3.39 (s, 3H), 3.49–3.60 (m, 2H), 3.97 (d, J = 7.6 Hz, 1H), 4.32 (dt, J = 7.8, 2.7 Hz, 1H), 4.58 (s, 1H), 5.24–5.27 (m, 2H), 5.63 (ddd, J = 10.3, 5.8, 2.0 Hz, 1H), 6.16 (dd, J = 10.3, 1.8 Hz, 1H), 6.58 (d, J = 2.5 Hz, 1H), 7.39 (d, J = 2.5 Hz, 1H); mass spectrum (APCI): *m/e* (% relative intensity) 606 (100) $(M+H)^+$, 588 (33) ($[M+H]^+$-H_2O), 570 (20), 548 (8) ($[M+H]^+$–*t*Bu), 530 (15), 512 (10), 475 (15).

21-*anti*: colorless thick oil; R_f = 0.20 (35% EtOAc in hexane); ^{1}H NMR (400 MHz, C_6D_6) δ 0.15 (s, 3H), 0.22 (s, 3H), 0.99 (d, J = 6.2 Hz, 3H), 1.01 (s, 9H), 1.07 (t, J = 7.1 Hz, 3H), 1.21 (s, 3H), 1.28 (t, J = 7.0 Hz, 3H), 1.30–1.40 (m, 1H), 1.52 (s, 3H), 1.52-1.62 (m, 1H), 1.93 (ddd, J = 15.0, 4.3, 3.1 Hz, 1H), 2.62 (ddd, J = 15.0, 12.0, 2.7 Hz, 1H), 2.96–3.05 (m, 1H), 3.26 (qd, J = 7.7, 1.1 Hz, 2H), 3.32 (s, 3H), 3.48–3.53 (m, 1H), 3.94 (d, J = 7.6 Hz, 1H), 4.00–4.09 (m, 1H), 4.28 (dt, J = 7.8, 2.5 Hz, 1H), 4.40 (s, 1H), 4.69 (dt, J = 12.1, 4.1 Hz, 1H), 5.60–5.64 (m, 2H), 6.06 (dd, J = 10.4, 1.9 Hz, 1H), 6.55 (d, J = 2.3 Hz, 1H), 7.20 (d, J = 2.3 Hz, 1H); mass spectrum (APCI): *m/e* (% relative intensity) 606

(100) $(M+H)^+$, 588 (25) ($[M+H]^+-H_2O$), 570 (15), 548 (7) ($[M+H]^+$-*t*Bu), 530 (10), 512 (8), 475 (15).

Data as mixture **21**-*syn* + **21**-*anti*: $[\alpha]_D^{20}=+24.3$ (*c* 0.070, C_6H_6); IR (neat) cm^{-1} 3430brm, 3242brm, 2936brm, 1767m, 1675m, 1606s, 1464s, 1257m, 1160s, 1023s, 840s; HRMS (ESI) calcd for $C_{32}H_{51}NO_8NaSi$ 628.3282, found 628.3287.

*Synthesis of lactone **22**-syn*

To a solution of alcohol **21**-*syn* (7.20 mg, 0.0119 mmol) in a ternary solvent mixture consisting of MeOH (0.6 mL), THF (0.2 mL), and H_2O (0.06 mL) was added KOH (6.70 mg, 0.119 mmol). The resulting mixture was stirred at rt overnight before being partitioned between H_2O (5 mL) and CH_2Cl_2 (5 mL). The mixture was extracted with CH_2Cl_2 (3 × 5 mL). The combined organic extracts were dried (Na_2SO_4) and concentrated *in vacuo* to give a crude oil that was purified via preparative TLC (eluted with 5% MeOH in CH_2Cl_2) to afford lactone **22**-*syn* in 71% yield (2.60 mg) as a thick oil along with the recovered but desilylated starting material (1.70 mg, 29%).

$R_f=0.75$ (5% MeOH in CH_2Cl_2); $[\alpha]_D^{20}=-37.9$ (*c* 0.68, $CHCl_3$); ^1H NMR (400 MHz, $CDCl_3$) δ 1.30 (d, $J=6.2$ Hz, 3H), 1.33 (s, 3H), 1.44 (s, 3H), 1.99 (ddt, $J=17.3$, 7.6, 3.0 Hz, 1H), 2.09–2.18 (m, 2H), 2.40 (ddd, $J=14.5$, 11.3, 3.1 Hz, 1H), 3.83 (s, 3H), 3.99–4.06 (m, 2H), 4.14 (d, $J=7.6$ Hz, 1H), 4.60 (dt, $J=7.6$, 2.7 Hz, 1H), 5.34 (d, $J=8.0$ Hz, 1H), 5.88 (dt, $J=10.3$, 2.0 Hz, 1H), 6.07 (ddd, $J=10.2$, 4.8, 3.3 Hz, 1H), 6.43 (d, $J=1.7$ Hz, 1H), 6.69 (d, $J=0.9$ Hz, 1H), 7.65 (br s, 1H); ^{13}C NMR (100 MHz, $CDCl_3$) δ 21.9, 24.5, 26.5, 27.5, 31.1, 56.1, 68.3, 70.2, 70.4, 74.9, 84.2, 95.5, 101.2, 103.0, 104.5, 109.4, 127.4, 127.8, 150.5, 157.7, 167.2, 171.9; IR (neat) cm^{-1} 2928w, 1733s, 1612s, 1480m, 1372m, 1320m, 1253m, 1213m, 1153s, 1032s, 849m; mass spectrum (APCI): m/e (% relative intensity) 419 (3) $(M+H)^+$, 401 (7), 361 (100), 343 (25), 317 (20), 167 (5); HRMS (ESI) calcd for $C_{22}H_{26}O_8Na$ 441.1525, found 441.1529.

*Synthesis of (+)-aigialospirol **4***

To a solution of lactone **22**-*syn* (28.0 mg, 0.067 mmol) in MeOH (4 mL) was added *p*-TsOH (2.70 mg, 0.014 mmol, practical grade). The mixture was stirred at rt for 4 h before it was concentrated *in vacuo* and diluted with CH_2Cl_2 (10 mL). The solution was washed with sat aq $NaHCO_3$ (10 mL). The aqueous layer was extracted with CH_2Cl_2 (3 × 10 mL), and the combined organic layers were dried (Na_2SO_4) and concentrated *in vacuo*. The resulting crude residue was purified via preparative TLC (eluted with 5% MeOH in CH_2Cl_2) to afford (+)-aigialospirol **4** in 53% yield (13.4 mg) as a white solid.

$R_f=0.49$ (5% MeOH in CH_2Cl_2); mp 90–94 °C; lit.[ref] 85–89 °C; $[\alpha]_D^{20}=+79.2$ (*c* 0.67, $CHCl_3$); lit.[ref] $[\alpha]_D^{25}=+47$ (*c* 0.50, $CHCl_3$); ^1H NMR (500 MHz, $CDCl_3$) δ 1.27 (d, $J=6.1$ Hz, 3H), 1.89 (ddd, $J=14.2$, 11.9, 2.6 Hz, 1H), 2.03–2.08 (m, 3H), 2.54 (d, $J=10.5$ Hz, 1H), 3.44 (d, $J=10.5$ Hz, 1H), 3.52 (dd, $J=9.9$, 3.3 Hz, 1H), 3.86 (s, 3H), 4.01 (m, 1H), 4.12–4.18 (m, 2H), 5.36 (d, $J=5.9$ Hz, 1H), 5.67 (dt, $J=10.0$, 2.0 Hz, 1H), 6.17 (dt, $J=10.0$, 4.0 Hz, 1H), 6.48 (d, $J=1.7$ Hz, 1H), 6.60 (s, 1H), 7.68 (s, 1H); ^{13}C NMR (100 MHz, $CDCl_3$) δ 21.1, 31.4, 33.6, 56.0, 65.0, 65.8, 68.3, 70.7, 82.3, 99.1, 101.2, 101.6, 104.3, 126.5, 130.5, 149.1, 157.7, 167.3, 171.3; IR ($CHCl_3$ film) cm^{-1} 3452brm, 3013w, 2970w, 2930w, 1736s, 1612s, 1444m, 1381m, 1316m, 1216m, 1154s, 1063s, 997s, 843w; mass spectrum (APCI): *m/e* (% relative intensity) 379 (15) $(M+H)^+$, 361 (100) $([M+H]-H_2O)^+$, 343 (25), 317 (12), 307 (10), 253 (37), 235 (16), 219 (7), 146 (98), 127 (10), 116 (7), 101 (30); HRMS (ESI) calcd for $C_{19}H_{22}O_8Na$ 401.1212, found 401.1208.

3 Results and discussion

3.1 Epimerization of the C6′ spiroketal carbon

Synthesis of key cyclic acetal RCM precursor commenced with δ-lactone **9**, which was prepared in grams quantity from *(S)*-glycidol in 6 steps [23, 27] (Scheme 3). A high yielding vinyl magnesium Grignard addition followed by acetalization using 1.0 equiv of Tf_2NH at −78 °C for 1 h [7, 9, 28] led to cyclic acetals **13** and **14** in 76% and 46% yield as a single diastereomer, respectively, from 3-butene-1-ol (as a model system), and chiral homo-allylic alcohol **12** [24, 25].

One distinct advantage of cyclic acetal tethered strategies for spiroketal synthesis is the high level of stereochemical control at the acetal carbon during the cyclic acetal construction, taking advantage of well-known anomerically favored axial addition in glycosylation chemistry [8, 29, 30]. However, nOe experiments on both **13** and **14** quickly confirm that while the stereoselectivity was very high in these cyclic acetal formations, the stereochemistry of the acetal carbon at C6′ is wrong. As shown in Figure 2, the homoallyloxy group at C6′ is actually alpha in **13** and **14**, thereby suggesting that the glycosylation process took place in an anti-anomeric manner via oxocarbenium ion **A**. The anomerically favored addition of ROH to **A** would have given the desired C6′ stereochemistry for (+)-aigialospirol (**4**).

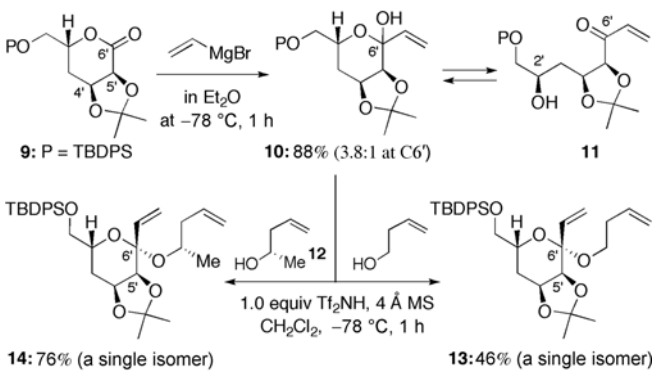

Scheme 3 Cyclic acetal RCM precursors.

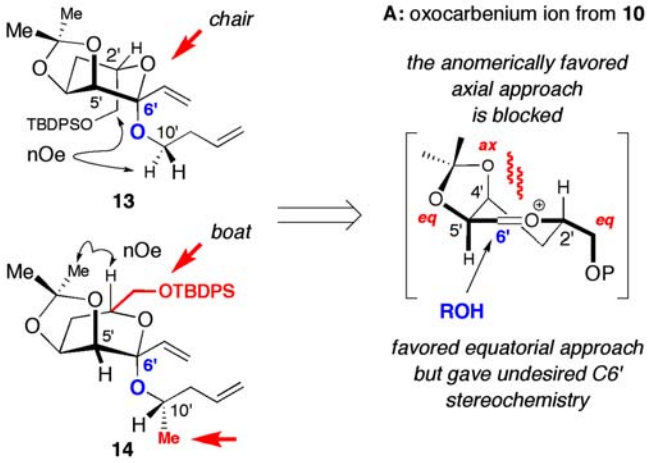

Figure 2 Stereochemistry of the cyclic acetal carbon C6′.

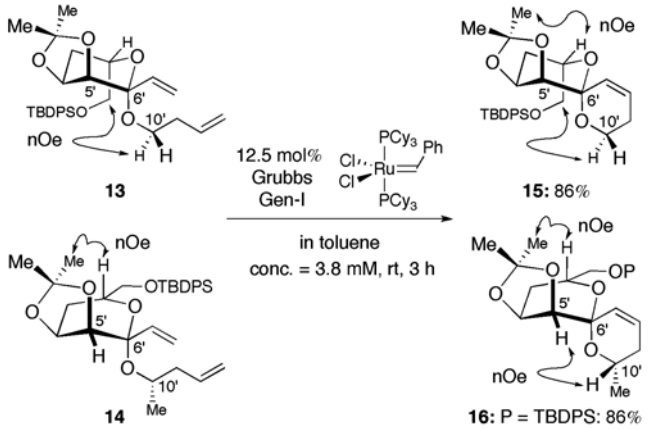

Scheme 4 The key cyclic acetal tethered RCM.

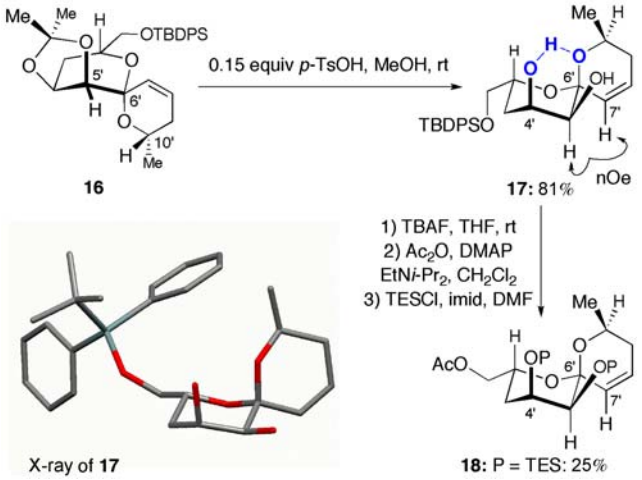

Scheme 5 Acid induced C6' epimerization.

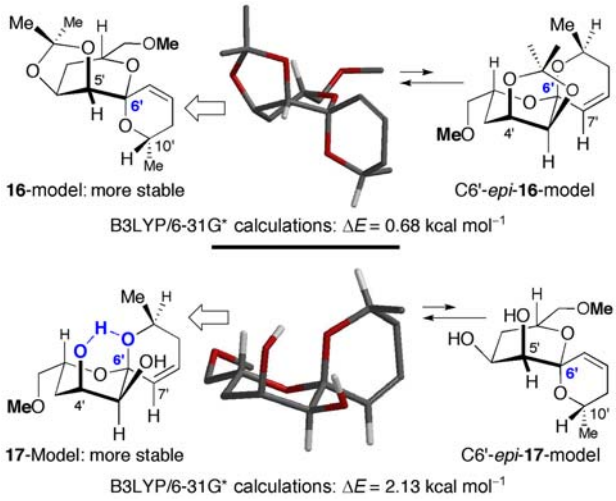

Figure 3 Energetics of **16**, **17** and their respective C6′ epimers.

This unexpected outcome is actually quite reasonable based on conformational considerations of oxocarbenium ion **A**, which would fit perfectly Woerpel's stereoelectronic model [29]: (a) The C2′ substituent could dominate by holding an equatorial position based on sterics; (b) the C–O bond at C4′ would be stereoelectronically favored to assume the equatorial position to minimize unfavorable $\sigma^*_{C\text{-}O}$ overlapping with the electron-deficient C6′ oxocarbenium carbon; and (c) the C–O bond at C5′ is also stereoelectronically favored to occupy the axial position. With these analyses, the anomerically favored axial entrance is completely blocked by the acetonide methyl group. It is also noteworthy that cyclic acetals **13** and **14** prefer two different conformations in the pyranyl ring, chair in the former and boat in the latter. This is likely due to the fact that the C10′ Me group in **14** would experience a greater 1,3-diaxial interaction (than that in **13**) with the C2′ methylene group when in a chair conformation.

Ring-closing metathesis of cyclic acetal **13** and **14** proceeded smoothly to give spiroketal **15** and **16** in 86% yield, respectively, employing 12.5 mol% Grubb's Gen-I catalyst (Scheme 4). Once again, nOe experiments on both **15** and **16** further confirmed that the stereochemistry at the C6′ spiroketal center is wrong in the context of (+)-aigialospirol **4** synthesis. In addition, while **15** tended to decompose under acidic conditions, removal the acetonide group in **16** using *p*-TsOH led to complete epimerization of stereocenter at the C6′ spiroketal carbon, as evident by both nOe and X-ray structure of diol **17** (Scheme 5).

B3LYP/6-31G* calculations [carried out using simplified model where the TBDPS group is replaced with Me group] revealed that the acetonide protected spiroketal **16** is actually 0.68 kcal mol^{-1} more stable than its corresponding C6′-epimer, whereas ΔE is 2.13 kcal mol^{-1} in favor of **17** over its C6′-epimer (Figure 3). Such a huge enhancement in the stability is likely a result of hydrogen bonding between C4′-OH and spiroketal oxygen, which was also seen in the X-ray structure and the minimized molecular model of **17**. It is noteworthy that the minimized conformational models of

16 and **17** are in close agreement with those predicted from nOe experiments (Scheme 4).

This key epimerization provided us with a window of opportunity to succeed in a total synthesis of (+)-aigialospirol **4** through diol **17**. However, the ensuing protecting group game using **17** was both messy and laborious (Scheme 5). In particular, the triol intermediate after removing the TBDPS group in **17** was difficult to handle given its polarity and water solubility. Fortuitously, B3LYP/6-31G* calculations once again demonstrate that the natural product (+)-aigialospirol **4** itself is also more stable than its C6′ epimer with a ΔE is 1.34 kcal mol^{-1} (Figure 4) presumably also experiencing the favourable hydrogen bonding between C4′-OH and spiroketal oxygen (blue arrow). Consequently, we elected to use **16** for the total synthesis and hoped to achieve a late stage C6′ epimerization under acidic conditions.

3.2 The unusual C1′-epimerization

As shown in Scheme 6, to continue our total synthesis effort, desilylation followed by oxidation of **16** gave aldehyde **19**. Snieckus' directed *ortho*-metallation [31] using amide **20** [26] proved to be a perfect protocol for assembling the benzolactone unit. Addition of **20**-Li afforded a readily separable mixture of alcohols **21**-*syn* and **21**-*anti* in 50% overall yield with an isomeric ratio 1:1.4.

Given the uncertainty of which isomer possesses the desired C1′-stereochemistry, both alcohols **21**-*syn* and **21**-*anti* were used for the lactone formation. However, during these investigations, it was found that **21**-*syn* and **21**-*anti* were actually epimerizing to one another. Specifically, pure **21**-*anti* was epimerizing to **21**-*syn* with prolonged exposure to silica gel. Therefore, to properly separate **21**-*syn* and **21**-*anti* via silica gel column chromatography, speed of the purification process actually mattered. Subsequently, epimerization of alcohol **21**-*anti* to **21**-*syn* was observed in C_6D_6 at rt. Most remarkably, epimerization was also occurring in frozen C_6D_6 at −10 °C with the final ratio arresting at 3:1 *syn:anti*, which matches the energetic differences attained using B3LYP/6-31G* calculations (carried out using simplified models where the TBS group is replaced with Me group) (Scheme 7).

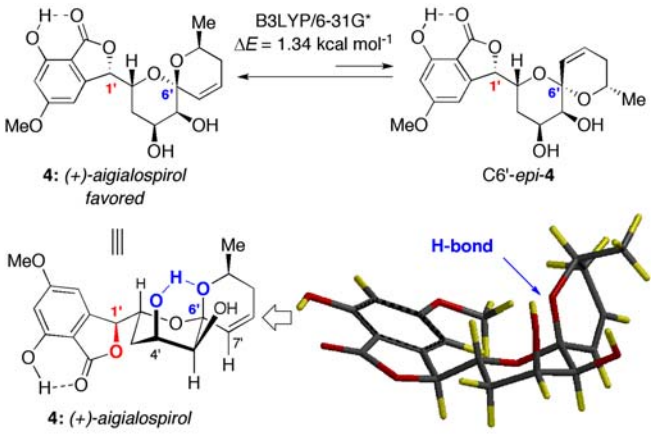

Figure 4 Energetics of (+)-aigialospirol **4** and C6′-*epi*-**4**.

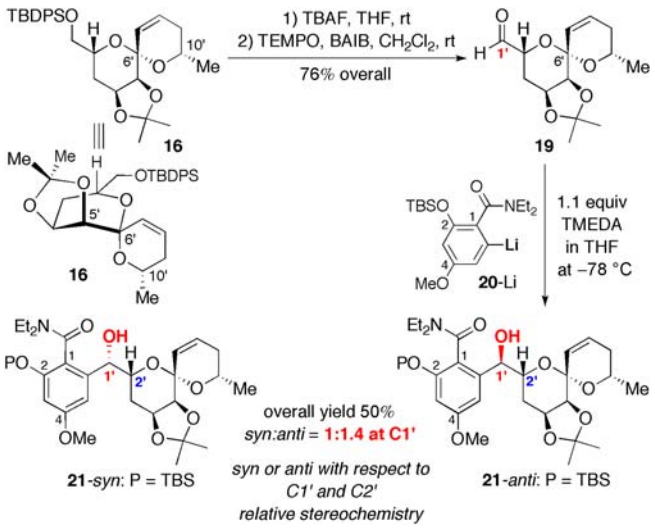

Scheme 6 Synthesis of epimeric C1′ alcohols via DOM.

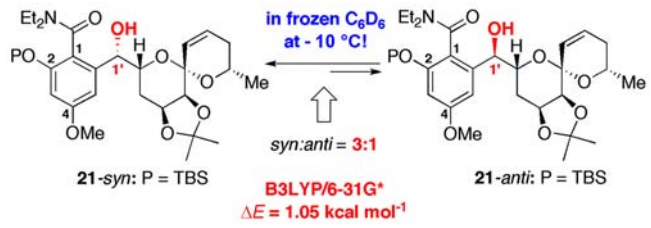

Scheme 7 Epimerization of **21**-syn and **21**-*anti* in frozen benzene.

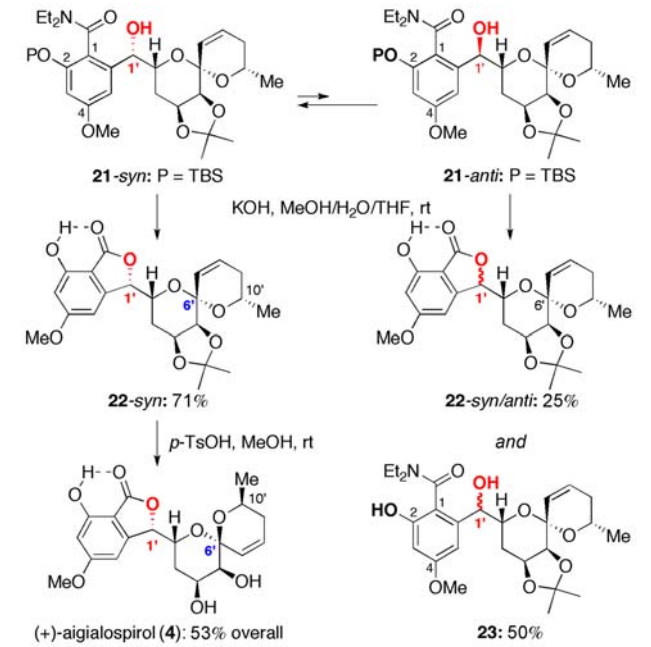

Scheme 8 Total synthesis of (+)-aigialospirol **4**.

To complete the total synthesis, lactone formation could be achieved using alkaline conditions at rt for 18 h, and alcohol **21**-*syn* gave lactone **22**-*syn* in 71% yield along with reacted starting material sans the TBS group (Scheme 8). On the other hand, while alcohol **21**-*anti* did indeed lactonize under the same conditions, the yield was very low. Most intriguingly, **21**-*anti* led to an isomeric lactone mixture **22**-*syn* and **22**-*anti* with a ratio of ~6:1 in favor of **22**-*syn*, and the major product was a ~1:1 mixture of **21**-*syn* and **21**-*anti* sans the TBS group. This outcome implies that **21**-*anti* was actually readily epimerizing to **21**-*syn* under basic conditions, and that the rate of lactonization for **21**-*syn* is greater than **21**-*anti*.

At last, as anticipated from earlier calculations (Figure 4), removal of the acetonide group in lactone **22**-*syn* took place concomitantly with the strategic C6' epimerization to afford (+)-aigialospirol **4** that matched the reported spectroscopic data [15].

3.3 Initial rationale for the C1′-epimerization

We were seriously intrigued by the C1′-epimerization because this epimerization involves the same C1′ stereocenter that is critical in the biosynthetic relationship between (+)-hypothemycin **7** and (+)-aigialospirol **4**. While acidic or basic conditions were not surprising given that C1′ is a benzylic carbon, the fact that epimerization took place in frozen benzene implies that the C1′-scrambling is remarkable and is likely intramolecular in nature.

The initial mechanistic proposal [23] involved the two diastereomeric pairs of hemi-*ortho*-aminal intermediates **24**-*syn-R* and **24**-*syn-S* and, and **24**-*anti-R* and **24**-*anti-S* as shown in Figure 5. The *R* and *S* designate stereochemistry of the C7 hemi-*ortho*-aminal carbon. A "turnstile-like" mechanism was postulated in which **24**-*syn-R* and **24**-*anti-S* could undergo swapping of the original C7 amido carbonyl oxygen atom (blue) with the C1′ hydroxy oxygen atom (red) [23].

A closer look through B3LYP/6-31G* calculations (carried out using simplified model where the TBS group is replaced with Me group) reveal that while **24**-*anti-S* is more stable than **24**-*anti-R,* for the *syn* isomeric pair, **24**-*syn-S* is actually more stable. However, unlike **24**-*syn-R*, **24**-*syn-S* is not suitable stereochemically for an intramolecular-like displacement at C1′ by the C7-OH group. Moreover, while analyzing the energetics of these hemi-*ortho*-aminal diastereomers may not be completely reflective of the actual mechanism because of the Curtin-Hammett principle, further modelling (Figure 6) reveals that stereoelectronically, the C7-OH group (blue arrow in **24**-*anti-S-model*) is not capable of such intramolecular displacement at C1′ (red dotted arrow in **24**-*anti-S-model*). This analysis firmly rules out our earlier mechanistic considerations.

3.4 C1′-epimerization via an imidanium ion-pair

What remain true are: (1) hemi-*ortho*-aminal diastereomers

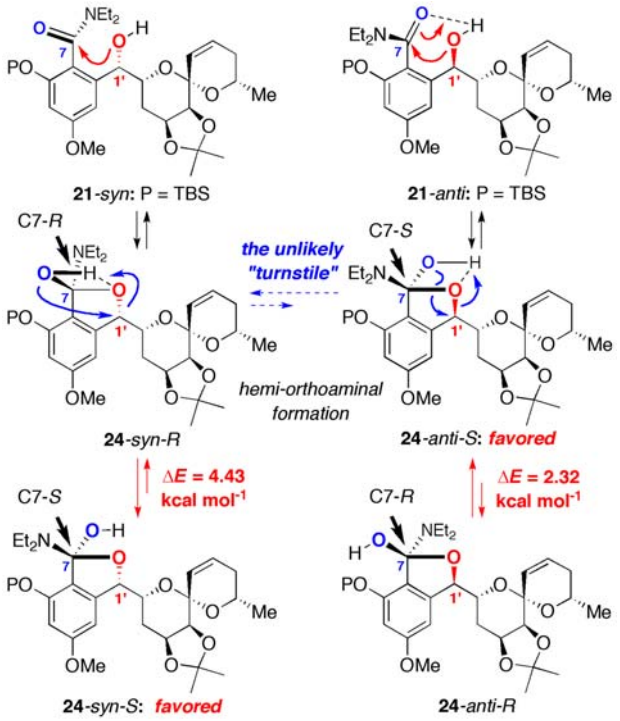

Figure 5 Initial thoughts for the C1′ epimerization.

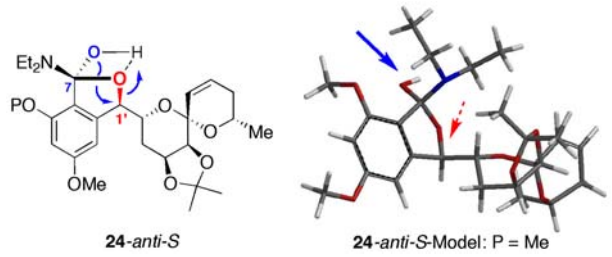

Figure 6 The turnstile-like mechanism unlikely.

have to be key intermediates; and (2) reaching **24**-*syn-S* from **21**-*syn* is likely faster than that of **21**-*anti* based on ΔE difference of 4.02 kcal mol^{-1} (B3LYP/6-31G*: P = Me as simplified models) between **24**-*syn-S and* **24**-*anti-S* (Figure 7). In addition, we continue to believe that C1′-epimerization is not a result of direct ionization at C1′ even under acidic conditions because the adjacent C2′ oxygen functionality would inductively disfavour this benzylic cation formation, and that the resorcinol ring cannot be supportive of this C1′-cation via resonance (inductively at best, albeit the C7–C=O group exerts the opposite effect).

However, another ionization process could take place in a highly plausible manner. As shown in Figure 7, imidanium ions **25**-*syn* and **25**-*anti* could be formed from **24**-*syn-S* and **24**-*anti-S*, respectively; or from **24**-*syn-R* and **24**-*anti-R*, respectively: not shown but cannot be ruled out [32]. This event renders the C1′ oxygen an excellent leaving group, allowing (a) intermolecular nucleophilic displacement under basic and/or acidic conditions; and (b) intramolecular-like

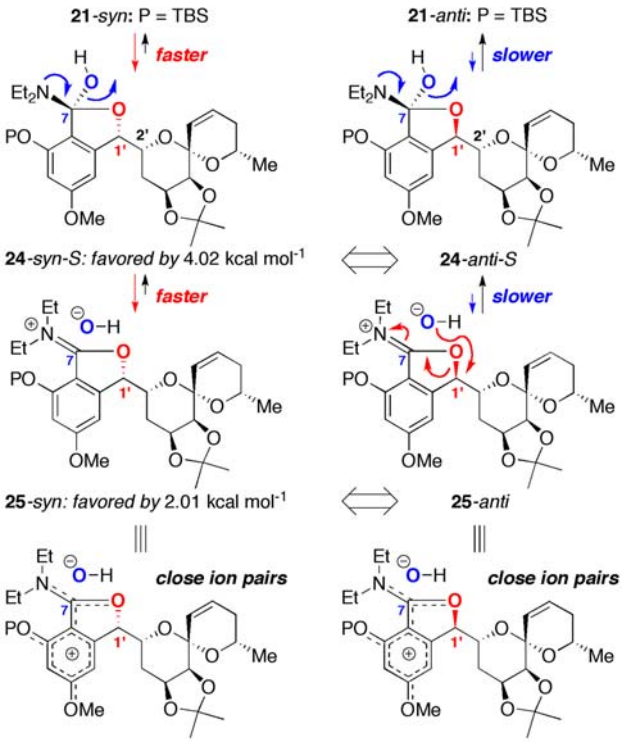

Figure 7 A more likely pathway for the C1′ epimerization.

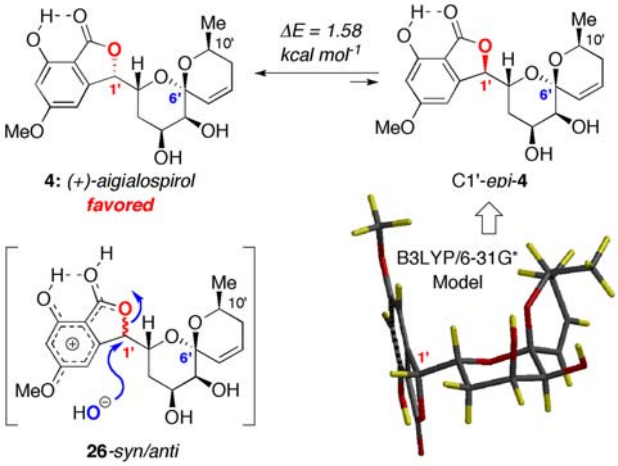

Scheme 9 Final assessment of C1′ stereochemistry in (+)-aigialospirol.

nucleophilic displacement in frozen benzene or neutral conditions, when **25**-*syn* and **25**-*anti* likely exist as close ion-pairs.

Most importantly, imidanium ions **25**-*syn* and **25**-*anti* are highly delocalized (see the overall resonance forms), and that **25**-*syn* is more stable than **25**-*anti* by 2.01 kcal mol^{-1} (B3LYP/6-31G*), thereby also suggesting the relative ease or faster rate of formation of **25**-*syn* from hemi-*ortho*-aminal **24**-*syn-S* (or *R*) over that of **25**-*anti*. Without calculating the actual activation energy, this assessment is consistent with the observation that **21**-*syn* underwent the intended lactonization quite rapidly to afford **22**-*syn* through most likely hydrolysis of imidanium ion **25**-*syn* (and/or hemi-*ortho*-aminal **24**-*syn-S*). On the other hand, the formation of imidanium ion **25**-*anti* from **21**-*anti* via **24**-*anti-S* is relatively sluggish. Consequently, the otherwise slower C1′-epimerization process, which is formally a S_N2 reaction on a highly hindered secondary carbocenter, is now allowed to compete favourably with hydrolysis.

Lastly, such C1′-epimerization implies that stereochemical integrity at C1′ of the natural product (+)-aigialospirol **4** itself could also be in jeopardy through an intermediate shown as **26**-*syn/anti* whether during the lactonization, during silica gel column purification, or being stored in non-polar/neutral solvents such as benzene (Scheme 9). However, calculations confirm that if such epimerization is occurring, C1′-*epi*-**4** is much less stable than **4** ($\Delta E = 1.58$ kcal mol^{-1} via B3LYP/6-31G*), thereby suggesting that the natural product (+)-aigialospirol **4** would dominate the equilibrium, and that the chance in detecting a significant amount of erosion of the stereochemical integrity at C1′ during either the isolation process or synthetic transformations would be slim.

In conclusion, we have described here two remarkable epimerization processes during our pursuit of an enantioselective synthesis of (+)-aigialospirol that featured a cyclic acetal tethered ring-closing metathesis. Through modeling, we were able to turn these two unexpected epimerizations to our advantage to ensure a successful and concise total synthesis, thereby firmly establishing cyclic acetal tethered RCM as a competitive and powerful strategy in natural product synthesis. More importantly, careful calculations allowed us to fully understand the nature and the mechanistic course of these two epimerizations.

Authors thank PRF-AC (42106) for support and Dr. Victor Young and Ben Kucera (University of Minnesota) for X-ray analysis. CCG thanks UW for an NIH-CBI Training Grant. We thank Professor Masahiko Isaka [National Center for Genetic Engineering and Biotechnology (BIOTEC), Pathumthani, Thailand] for kindly providing the original spectra data of (+)-aigialospirol.

1 For a reviews, see; (a) Mukaiyama T, Murakami M. Cross-coupling reactions based on acetals. *Synthesis,* 1987: 1043–1054; (b) Alexakis A, Mangeney P. Chiral acetals in asymmetric synthesis. *Tetrahedron Asy*, 1990, 1: 477–511
2 Also see: Harmata M, Rashatasakhon P. Cycloaddition reactions of vinyl oxocarbenium ions. *Tetrahedron*, 2003, 59: 2371–2395
3 Ko C, Feltenberger JB, Ghosh SK, Hsung RP. Gassman's intramolecular [2+2] cationic cycloaddition. Formal total syntheses of raikovenal and *epi*-raikovenal. *Org Lett*, 2008, 10: 1971–1974
4 For reviews, see: (a) Aho JE, Pihko PM, Rissa TK. Nonanomeric spiroketals in natural products: Structures, sources, and synthetic Strategies. *Chem Rev*, 2005, 105: 4406–4440; (b) Mead KT, Brewer BN. Strategies in spiroketal synthesis revisited: Recent applications and advances. *Curr Org Chem*, 2003, 7: 227–256; (c) Brimble MA, Fares FA. Synthesis of bis-spiroacetal ring systems. *Tetrahedron*, 1999, 55: 7661–7706; (d) Fletcher MT, Kitching W. Chemistry of fruit flies. *Chem Rev,* 1995, 95: 789–828; (e) Perron F, Albizati KF. Chemistry of spiroketals. *Chem Rev*, 1989, 89: 1617–1661

5 For cyclic acetal tethered IMDA, see: Wang J, Hsung RP, Ghosh SK. Stereoselective ketal-tethered intramolecular Diels-Alder cycloadditions. An approach to the 2-oxadecalin spiroketal core of antifungal agent *Fusidilactone C*. *Org Lett*, 2004, 6: 1939–1942

6 For cyclic acetal tethered Pauson-Khand, see: Ghosh SK, Hsung RP, Liu J. An anomeric control on remote stereochemistry in the synthesis of spiroketals. *J Am Chem Soc*, 2005, 127: 8260–8261

7 For cyclic acetal tethered RCM, see: (a) Ghosh SK, Hsung RP, Wang J. Ketal-tethered ring-closing metathesis. An unconventional approach to constructing spiroketals and total synthesis of an insect pheromone. *Tetrahedron Lett*, 2004, 45: 5505–5510; (b) Ghosh SK, Ko C, Liu J, Wang J, Hsung RP. A ketal-tethered RCM strategy toward the synthesis of spiroketal related natural products. *Tetrahedron*, 2006, 62: 10485–10496

8 For reviews, see: (a) Postema MHD. Recent developments in the synthesis of *C*-glycoside. *Tetrahedron,* 1992, 48: 8545–8599; (b) Postema MHD. *C-Glycoside Synthesis*. Ann Arbor: CRC Press, 1995; (c) Parker KA. Novel methods for the synthesis of *C*-aryl glycoside natural products. *Pure Appl Chem*, 1994, 66: 2135–2138; (d) Levy DE, Tang C. *The Chemistry of C-Glycosides*, 1st ed. Pergamon Press. 1995, Vol. 13

9 Ko C, Hsung RP. An unusual stereoselectivity in the anomeric substitution with carbamates promoted by $HNTf_2$. *Org Biomol Chem,* 2007, 7: 431–434

10 For RCM, see: (a) Leeuwenburgh MA, Appeldoorn CCM, Van Hooft PAV, Overkleeft HA, Van der Marel GA, Van Boom JH. Synthesis of highly functionalized carbohydrate-derived spiroacetals by ring-closing metathesis and Pauson-Khand reaction of ketoglycosidic enynes. *Eur J Org Chem*, 2000: 837–877; (b) Bassindale MJ, Hamley P, Leitner A, Harrity JPA. Spirocycle assembly through selective tandem ring closing metathesis reactions. *Tetrahedron Lett*, 1999, 40: 3247–3250; (c) Donnard M, Tschamber T, Desrat S, Hinsinger K, Eustache J. Ring-rearrangement metathesis of 3,6-dialkoxy-3,6-dihydro-2*H*-pyrans. *Tetrahedron Lett*, 2008, 49: 1192–1195

11 For [2+2+2] cycloadditions, see: Yamamoto Y, Hashimoto T, Hattori K, Kikuchi M, Nishiyama H. Synthesis of spirocyclic *C*-arylribosides via cyclotrimerization. *Org Lett*, 2006, 8: 3565–3568

12 For other related RCM templated by acetals, see: (a) Scholl M, Grubbs RH. Total synthesis of (−)- and (±)-frontalin via ring-closing metathesis. *Tetrahedron Lett*, 1999, 40: 1425–1428; (b) Keller VA, Martinelli JR, Strieter ER, Burke SD. Dioxolane-to-bridged acetal-to-spiroketal via ring-closing metathesis and rearrangement: A novel route to 1,7-dioxaspiro[5.5]undecanes. *Org Lett*, 2002, 4: 467–470; (c) Voight EA, Rein C, Burke SD. Synthesis of sialic acids via desymmetrization by ring-closing metathesis. *J Org Chem*, 2002, 67: 8489–8499; (d) Burke SD, Voight EA. Formal synthesis of (+)-3-deoxy-D-glycero-D-galacto-2-nonulosonic acid (KDN) via desymmetrization by ring-closing metathesis. *Org Lett,* 2001, 3: 237–240; (e) Burke SD, Muller N, Beaudry CM. Desymmetrization by ring-closing metathesis leading to 6,8-dioxabicyclo[3.2.1]octanes: A New route for the synthesis of (+)-exo- and endo-brevicomin. *Org Lett*, 1999, 1: 1827–1829; (f) Kinderman SS, Doodeman R, Van Beijma JW, Russcher JC, Tjen KCMF, Kooistra TM, Mohaselzadeh H, Van Maarseveen JH, Hiemstra H, Schoemaker HE, Rutjes FPJT. Ring-closing metathesis of allylic *O,O*- and *N,O*-acetals. *Adv Syn Catal*, 2002, 344: 736–748

13 For recent reviews, see: (a) Trnka TM, Grubbs RH. The development of L2X2Ru:CHR olefin metathesis catalysts: An organometallic success story. *Acc Chem Res*, 2001, 34, 18–29; (b) Hoveyda AH, Schrock RR. Catalytic asymmetric olefin metathesis. *Chem Eur J*, 2001, 7: 945–950; (c) Walters MA. Recent advances in the synthesis of heterocycles via ring-closing metathesis. *Prog Heteroc Chem*, 2003, 15: 1–36; (d) Nakamura I, Yamamoto Y. Transition-metal-catalyzed reactions in heterocyclic synthesis. *Chem Rev*, 2004, 104: 2127–2198; (e) Deiters A, Martin SF. Synthesis of oxygen- and nitrogen-containing heterocycles by ring-closing metathesis. *Chem Rev,* 2004, 104: 2199–2238; (f) McReynolds MD, Dougherty JM, Hanson PR. Synthesis of phosphorus and sulfur heterocycles via ring-closing olefin metathesis. *Chem Rev*, 2004, 104: 2239–2258; (g) Wallace DJ. Relay ring-closing metathesis – A strategy for achieving reactivity and selectivity in metathesis chemistry. *Angew Chem Int Ed*, 2005, 44: 1912–1915

14 For application in spirastrellolide A synthesis, see: (a) Liu J, Hsung RP. Synthesis of the C11–C23 fragment of spirastrellolide A. A ketal- tethered rcm approach to the construction of spiroketals. *Org Lett*, 2005, 6: 2273–2276; (b) Yang J-H, Liu J, Hsung RP. Synthesis of the C1-C23 fragment of spirastrellolide A. *Org Lett*, 2008, 10: 2525–2528

15 Vongvilai P, Isaka M, Kittakoop P, Srikitikulchai, P, Kongsaeree P, Thebtaranonth Y. Ketene acetal and spiroacetal constituents of the marine fungus *Aigialus parvus* BCC 5311. *J Nat Prod*, 2004, 67: 457–460

16 For biological activities of marine fungi in general, see: Faulkner DJ. Marine natural products. *Nat Prod Rep*, 2001, 18: 1–49

17 (a) Nair MSR, Carey ST. Metabolites of pyrenomycetes. XIII. Structure of (+)-hypothemycin, an antibiotic macrolide from Hypomyces trichothecoides. *Tetrahedron Lett*. 1980, 21: 2011–2012; (b) Nair MSR, Carey ST, James JC. Metabolites of pyrenomycetes. XIV. Structure and partial stereochemistry of the antibiotic macrolides hypothemycin and dihydrohypothemycin. *Tetrahedron*, 1981, 37: 2445–2449

18 Revised structure of hypothemycin: Agatsuma T, Takahashi A, Kabuto C, Nozoe S. Revised structure and stereochemistry of hypothemycin. *Chem Pharm Bull*, 1993, 41: 373–375

19 For a leading review on syntheses of hypothemycin and related resorcylic macrolides, see: Winssinger N, Barluenga S. Chemistry and biology of resorcylic acid lactones. *Chem Commun*, 2007: 22–36

20 For a total synthesis of hypothemycin, see: (a) Selles P, Lett R. Convergent stereospecific synthesis of C292 (or LL-Z1640-2), and hypothemycin. Part 1. and Convergent stereospecific synthesis of LL-Z1640-2 (or C292), hypothemycin and related macrolides. Part 2. *Tetrahedron Lett*, 2002, 43: 4621–4625, and 4627-4631; For syntheses of other related resorcylic macrolides, see: (b) Yang ZQ, Geng X, Solit D, Pratilas CA, Rosen N, Danishefsky SJ. New efficient synthesis of resorcinylic macrolides via ynolides: Establishment of cycloproparadicicol as synthetically feasible preclinical anticancer agent based on Hsp90 as the Target. *J Am Chem Soc*, 2004, 126, 7881–7889; (c) Barluenga S, Dakas PY, Ferandin Y, Meijer L, Winssinger N. Modular asymmetric synthesis of aigialomycin D, a kinase-inhibitory scaffold. *Angew Chem Int Ed*, 2006, 45: 3951–3954; (d) Lu J, Ma J, Xie X, Chen B, She X, Pan X. Enantioselective total synthesis of aigialomycin D. *Tetrahedron Asy*, 2006, 17: 1066–1073; (e) Grosche P, Akyel K, Marzinzik A. Synthesis of macrocyclic scaffolds from natural products and their utilization for solid-phase chemistry. *Synthesis*, 2005: 2015–2021; (f) Garbaccio RM, Stachel SJ, Baeschlin DK, Danishefsky SJ. Concise asymmetric syntheses of radicicol and monocillin I. *J Am Chem Soc*, 2001, 123: 10903–10908; (g) Lampilas M, Lett R. Convergent stereospecific total synthesis of monochiral monocillin I related macrolides. And convergent stereospecific total synthesis of monocillin I and monorden (or radicicol). *Tetrahedron Lett*, 1992, 33: 773–776 and 777–780

21 Isaka M, Suyarnsestakorn C, Tanticharoen M, Kongsaeree P, Thebtaranonth Y. Aigialomycins A–E, new resorcylic macrolides from the marine mangrove fungus *Aigialus parvus*. *J Org Chem*, 2002, 67, 1561–1566

22 (a) Tanaka H, Nishida K, Sugita K, Yoshioka T. Antitumor efficacy of hypothemycin: A new ras-signaling inhibitor. *Jpn J Cancer Res*, 1999, 90: 1139–1145; (b) **S**chirmer A, Kennedy J, Murli S, Reid R, Santi DV. Targeted covalent inactivation of protein kinases by resorcylic acid lactone polyketides. *Proc Nat Aca Sci*, 2006, 103: 4234–4239

23 Figueroa R, Hsung RP, Guevarra CC. An enantioselective total synthesis of (+)-aigialospirol. *Org Lett*, 2007, 9, 4857–4859.

24 Marshall JA, Sabatini JJ. Synthesis of *cis*- and *trans*-2,5-disubstituted tetrahydrofurans by a tandem dihydroxylation-S_N2 cyclization sequence. *Org Lett*, 2005, 7: 4819–4822

25 Kumar P, Gupta P, Naidu SV. A simple and efficient approach to 1,3-polyols: application to the synthesis of cryptocarya diacetate. *Chem Eur J*, 2006, 12: 1397–1402

26 Prepared by following Sellès' conditions: (a) See reference [20a]; (b) Wissner A, Grudzinskas C. Reaction of *tert*-butyldimethylsilyl esters with oxalyl chloride-dimethylformamide: Preparation of carboxylic acid chlorides under neutral conditions. *J Org Chem*, 1978, 43: 3972–3974

27 Hansen TV. Synthesis of (*R*)-(−)-argentilactone. *Tetrahedron Asy*, 2002, 13: 547–550

28 For leading references on using $HNTf_2$, see: (a) Sakakura A, Suzuki K, Nakano K, Ishihara K. Chiral 1,1′-Binaphthyl-2,2′-diammonium salt catalysts for the enantioselective Diels-Alder reaction with. alpha.-acyloxyacroleins. *Org Lett*, 2006, 8: 2229–2232; (b) Sun J, Kozmin SA. Bronsted acid-promoted cyclizations of 1-siloxy-1,5-diynes. *J Am Chem Soc*, 2005, 127, 13512–13513; For the acidity of $HNTf_2$, see: (c) Thomazeau C, Olivier-Bourbigou H, Magna L, Luts S, Gilbert B. Determination of an acidic scale in room temperature ionic liquids. *J Am Chem Soc*, 2003, 125: 5264–5265, and references cited therein.

29 (a) Shenoy SR, Smith DM, Woerpel KA. Nucleophilic additions of trimethylsilyl cyanide to cyclic oxocarbenium ions: Evidence for the loss of stereoselectivity at the limits of diffusion control. *J Am Chem Soc*, 2006, 128, 8671–8677; (b) Smith DM, Woerpel KA. Using stereoelectronic effects to explain selective reactions of 4-substituted five-membered ring oxocarbenium ions. *Org Lett*, 2004, 6: 2063–2066; (c) Romero JAC, Tabacco SA, Woerpel KA. Stereochemical reversal of nucleophilic substitution reactions depending upon substituent: Reactions of heteroatom-substituted six-membered-ring oxocarbenium ions through pseudoaxial conformers. *J Am Chem Soc*, 2000, 122, 168–169; (d) Matsutani H, Ichikawa S, Yaruva J, Kusumoto T, Hiyama T. Synthesis and Lewis acid-catalyzed nucleophilic substitution of chiral 1-alkoxyalkyl carboxylates. *J Am Chem Soc*, 1997, 119: 4541–4542; (e) Hosokawa S, Kirschbaum B, Isobe M. 1,4-Anti induction in *C*-glycosylation of pentose glycals. *Tetrahedron Lett*, 1998, 39: 1917–1920

30 (a) Woods RJ, Andrews CW, Bowen JP. Molecular mechanical investigations of the properties of oxocarbenium ions. 2. Application to glycoside hydrolysis. *J Am Chem Soc*, 1992, 114: 859–864; (b) Miljkovic M, Yeagley D, Deslongchamps P, Dory YL. Experimental and theoretical evidence of through-space electrostatic stabilization of the incipient oxocarbenium ion by an axially oriented electronegative substituent during glycopyranoside acetolysis. *J Org Chem*, 1997, 62: 7597–7604

31 (a) Snieckus V. Heterocycles via *ortho*-lithiated benzamides. *Heterocycles* 1980, 14: 1649–1676; (b) Beak P, Snieckus V. Directed lithiation of aromatic tertiary amides: An evolving synthetic methodology for polysubstituted aromatics. *Acc Chem Res*, 1982, 15: 306–312; (c) Snieckus V. Directed ortho metalation. Tertiary amide and O-carbamate directors in synthetic strategies for polysubstituted aromatics. *Chem Rev*, 1990, 90: 879–933; (d) Anctil EJ.-G, Snieckus V. The directed ortho metalation-cross coupling symbiosis. Regioselective methodologies for biaryls and heterobiaryls. Deployment in aromatic and heteroaromatic natural product synthesis. *J Organomet Chem*, 2002, 653: 150–160

32 One of the referees kindly pointed out a third approach that could account for either the observed epimerization through the direct formation of the proposed imidanium ion pairs. This insightful suggestion is also plausible and cannot be ruled out especially under the acidic conditions. While it places less significance on the hemi-*ortho*-aminal formation, it accentuates the importance of the amido-group and implies that such epimerization may not take place in the absence of the amido-group